PAPER

NJC
www.rsc.org/njc

Molecular photosensors of self-assembled monolayers: electron acceptor–photosensitizer dyad on an ITO surface

Kyung-Hee Hyung,†[a] Dong-Young Kim[b] and Sung-Hwan Han*[a]

[a] *Department of Chemistry, Hanyang University, Haengdang-dong 17, Sungdong-ku, Seoul, Korea 133-791. E-mail: shhan@hanyang.ac.kr; Fax: +822-2299-0762; Tel: +822-2290-0934*
[b] *Opto-Electronic Materials Research Center, Korea Institute of Science and Technology, 39-1, Hawolgok-dong, Seongbuk-gu, Seoul, Korea 136-791*

Received (in Montpellier, France) 15th February 2005, Accepted 26th May 2005
First published as an Advance Article on the web 5th July 2005

Self-assembled monolayers of di-(3-diaminopropyl)-viologen (DAPV) were prepared on a tin-doped indium oxide (ITO) surface as acceptor layers. Photoactive layers of Ru(2,2′-bipyridine-4,4′-dicarboxylic acid)$_2$(NCS)$_2$ were formed on DAPV to give an acceptor–sensitizer dyad on ITO. The photon energy was monitored by measuring the ITO conductivity change. Under illumination, the ITO conductivity increased with the current increasing by increments of 8 nA indicating the construction of molecular photosensors on the ITO surface. The concept of a molecular photosensor was further applied to a molecular photovoltaic system. The presence of the viologen moiety bridges the energy levels between the LUMO of the Ru sensitizer and ITO, and improves the efficiency of a photovoltaic cell with a quantum yield of 18.4% at 3.3 mW cm^{-2}.

Introduction

The photosynthesis system provides insight into the emerging fields of photosensors, photovoltaics, and opto-electronic devices.[1–5] Photosynthesis consists of a two-photon excitation system, P680 and P700, and an electron acceptor system with quinone and ferredoxine.[6] The acceptor–sensitizer–donor system in nature is efficiently arranged three dimensionally as well as energetically, which sets up the basis for a high efficiency photosynthetic system.[7–10] In order to mimic the photosynthesis, the design and construction of molecular architectures of acceptors, donors and photoresponsive materials on ITO (tin-doped indium oxide) is quite necessary.

Self-assembled monolayers (SAMs) on gold and platinum have been studied extensively. Nonetheless, metal films are not optically transparent, and the SAMs on them are not chemically stable. Since the first report on SAMs of diamine molecules on ITO, molecular layering on ITO has attracted a great deal of attention for photoelectrochemical applications.[11–15] The SAMs on ITO can get rid of the limitations of SAMs on Au and provide stable and versatile applications.

In the work described in this paper, we intended to construct an acceptor–sensitizer molecular dyad architecture on the ITO surface, which has a strong potential to be applied to photovoltaic systems. We report the preparation of a molecular photosensor on an ITO surface mimicking photosynthesis in nature. Self-assembled monolayers of di-(3-diaminopropyl)-viologen (DAPV) and Ru(2,2′-bipyridine-4,4′-dicarboxylic acid)$_2$(NCS)$_2$ were constructed on an ITO surface to give an acceptor–sensitizer dyad on ITO. The photon energy was monitored by measuring the ITO conductivity change in the presence of the dyad on its surface. Upon illumination, the ITO conductivity changed along with a current increase. The formation of an acceptor–sensitizer dyad on ITO successfully provided an efficient route for molecular photosensors. This system was further applied to electric current generation/photovoltaics in the presence of $I^-/I_3^-/CH_3CN$. Grätzel's photovoltaic system uses TiO_2 as an electron acceptor. Nanoparticles of semiconductor solid oxide layers are deposited on the ITO surface followed by the adsorption of dye. The SAMs of organic molecules successfully constitute an electron acceptor system with an excellent quantum yield of 18.4% at 3.3 mW cm^{-2}.

† Supported by the Brain Korea 21 Project in 2003.

Experimental

High purity water (Milli-Q, Millipore) was used for all experiments. All of the chemicals were purchased from Aldrich. Ru(2,2′-bipyridine-4,4′-dicarboxylic acid)$_2$(NCS)$_2$ was purchased from Solaronix. Di-(3-diaminopropyl)-viologen (DAPV) was synthesized with 4,4-bipyridine and 3-bromopropylamine hydrobromide by refluxing for 12 h. ITO (10 Ω cm) glass was purchased from Samsung Corning Co. and HOYA Co. The self-assembled monolayers of 1,12-diaminododecane (DADD) on ITO were prepared by immersing the ITO in 2 mM DADD in methanol at 40 °C under an Ar atmosphere for 48 h. The self-assembled monolayers of DAPV on ITO were prepared by immersing the ITO in 2 mM DAPV in 0.1 M phosphate buffer, pH 7.0 at 40 °C for 48 h. The layer of $RuL_2(NCS)_2$ was prepared by dipping SAMs–ITO in 0.3 mM Ru complex–ethanol solution for 24 h. To monitor the conductivity of ITO, high resistance ITO (1 kΩ cm) was used, and the dyad was formed by the procedure mentioned above.

The electrochemical measurements were performed using a BAS 100B (Bioanalytical Systems, Inc.). A single compartment with a standard three-electrode glass cell was used with Ag/AgCl as a reference electrode and Pt wire as a counter electrode. The measurement in aqueous media was carried out under an Ar atmosphere. In order to calculate the surface concentration of phosphomolybdic acid, cyclic voltammetry (CV) was performed: the cyclic voltammogram of bare ITO in a 0.1 M HCl solution was obtained as a blank test and baseline. Then, the cyclic voltammogram of phosphomolybdic acid–SAMs on the ITO surface was overlapped on the base line,

DOI: 10.1039/b502353j

and the second reduction peak was integrated to calculate the amount of electron transfer. Cyclic voltammetry was also carried out to characterize and calculate the surface concentration of $RuL_2(NCS)_2$ on SAMs–ITO. Cyclic voltammetry was carried out under an Ar atmosphere (0.1 M $(Bu)_4NBF_4$–CH_3CN, scan rate, 50 mV s^{-1}; air mass 0 and 1.5 filter systems and light of 25 mW cm^{-2} and 0.4 cm^2 irradiation area).

The spectroscopic measurements were carried out using Rutherford backscattering spectroscopy (RBS, which was performed at the KIST–RBS facility with a 2 MeV He^{2+} ion source), and UV-spectroscopy (Varian, CARY100 spectrophotometer).

The $RuL_2(NCS)_2$–DAPV dyad was prepared by dipping the SAMs–ITO (1 kΩ cm) in 0.3 mM Ru complex–ethanol solution for 24 h, and a silver paste was applied at the edge for the electrical contact. SAMs of dyad–ITO (1.5 × 2.5 cm^2) were illuminated with 89 mW cm^{-2} white light with air mass 0 and 1.5 filters as a solar simulator in the presence of a water filter (450 W Xenon lamp, Oriel Instruments). Current was measured at 0.05 mV by a Kiethley 2400 source meter in air or in a vacuum (10^{-6} Torr.). The two-probe method was used to monitor the change in the conductivity/resistivity efficiently.

A sandwich-type photovoltaic cell was assembled with $RuL_2(NCS)_2$–DAPV–ITO and Pt-sputtered ITO glass [electrolyte: 0.3 M LiI and 30 mM I_2 in $(Bu)_4NBF_4$–CH_3CN, 0.34 cm^2]. Photocurrent action spectra were measured by changing the excitation wavelength ($\Delta\lambda$ = 2 nm) (photon counting spectrometer, ISS Inc. and Kiethley 2400 source meter). The *J–V* characteristics of the cell were carried out using Kiethley 2400 source meter under λ = 530 nm and 3.3 mW cm^{-2}. The light intensity was tuned with an optical power meter (Newport Co.). Quantum yields were calculated based on the number of photons absorbed by the sensitizer at 530 nm $\{\Phi = [(hc/e)J_{sc}]/[\lambda I(1 - 10^{-A})]$; *h*, Planck constant; *c*, speed of light; *e*, electron charge; J_{sc}, photocurrent density; λ, wavelength of excitation light; *I*, light intensity irradiated at λ nm; *A*, absorbance of the sensitizer on SAMs–ITO at λ nm$\}$.

Results and discussion

(1) Self-assembled monolayers of di-(3-diaminopropyl)-viologen on ITO and molecular layering of Ru(2,2′-bipyridine-4,4,-dicarboxylic acid)$_2$(NCS)$_2$ on SAMs–ITO

SAMs of di-(3-diaminopropyl)-viologen were prepared on an ITO surface using the previously reported method.[11–15] The SAMs were quite stable in air and even survived in 0.1 N HCl solution. As a reference, SAMs of diaminododecane were prepared on ITO, too. The formation of DAPV SAMs on ITO was monitored by the cyclic voltammetry (Fig. 1). Viologen is well known to give two characteristic redox peaks in cyclic voltammogram in solution. However, on the ITO surface, SAMs of viologen form the dimer $[(DAPV^{\bullet+})_2]$ with one electron reduction.[16–18] The first reduction peak at −532 mV is related to formation of a dimer from $DAPV^{2+}$, and the second one at −960 mV, $DAPV^{\bullet+/0}$. The surface concentrations of DAPV and DADD on the ITO were quantified using cyclic voltammetry of the phosphomolybdic acid ($H_3PMo_{12}O_{40}$) adsorbed on the amine layers by the formation of an acid–base complex (Scheme 1).[11,15] Phosphomolybdic acid is a strong Brønsted acid with multi-protons, and easily forms monolayers on the basic DAPV on ITO. Phosphomolybdic acid has good redox properties and has been investigated for its electrochemical behavior. The phosphomolybdic acid undergoes multiple electron transfers in solution (Fig. 2). All the electrochemical measurements showed good reproducibility within an error range of 10%. The surface concentration of phosphomolybdic acid was measured by integrating the reduction current. The surface concentrations of DAPV and DADD were characterized to give 4.3 × 10^{-10} and 4.2 × 10^{-10} mol cm^{-2}, respectively.

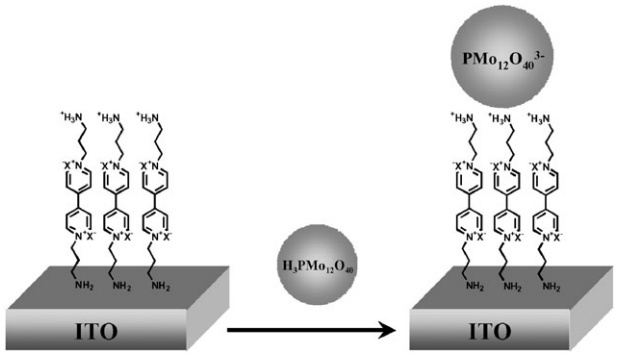

Scheme 1 The formation of di-(3-diaminopropyl)-viologen (DAPV) SAMs and acid–base complex between DAPV and phosphomolybdic acid.

The amine functional group was utilized to form a second layer of Ru(2,2′-bipyridine-4,4,-dicarboxylic acid)$_2$(NCS)$_2$ [$RuL_2(NCS)_2$] as a photosensitizer by forming an acid–base complex on SAMs. The quantitative measurements of $RuL_2(NCS)_2$ on SAMs–ITO were carried out using cyclic voltammetry to give 4.7 × 10^{-10} mol cm^{-2} on DAPV and 4.3 × 10^{-10} mol cm^{-2} on DADD by integrating the character-

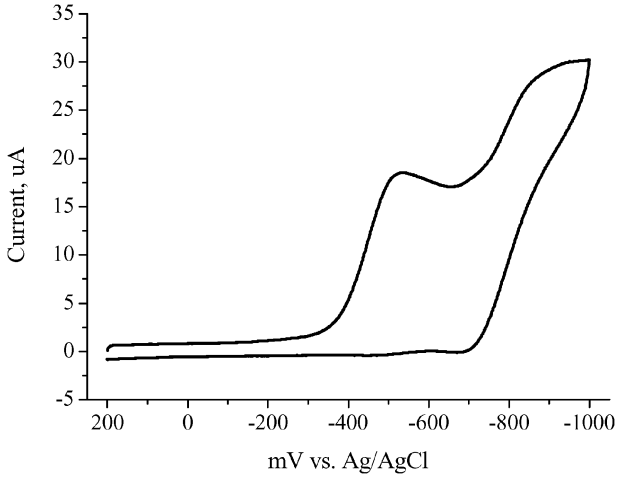

Fig. 1 Cyclic voltammogram of DAPV–ITO in electrolyte, 0.1 M $(Bu)_4NBF_4$–CH_3CN. Scan rate, 50 mV s^{-1}.

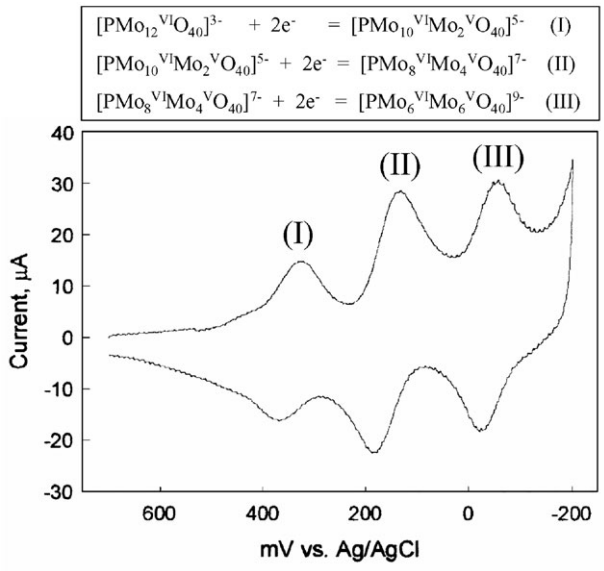

Fig. 2 Cyclic voltammogram of phosphomolybdic acid on DAPV–ITO in 0.1 M HCl at 200 mV s^{-1}.

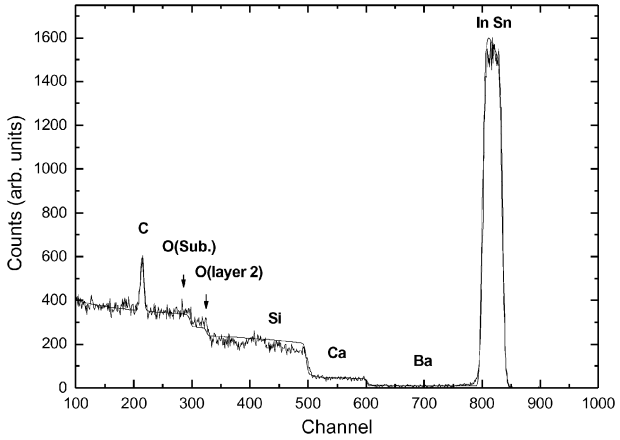

Fig. 3 Rutherford backscattering spectrum of di-(3-diaminopropyl)-viologen on ITO.

istic ruthenium oxidation signal in a cyclic voltammogram. The surface concentrations of ruthenium and the SAMs were measured independently by counting the carbon signals in the Rutherford backscattering spectra (Fig. 3): DADD, 9.0×10^{-10}; DAPV, 8.8×10^{-10}; $RuL_2(NCS)_2$ on DAPV, 7.4×10^{-10} mol cm^{-2}, respectively (Fig. 2b).[11,12,15] The surface concentrations that were obtained by integrating the phosphomolybdic acid signals in the cyclic voltammograms were the minimum values. On the other hand, the RBS data gave the maximum values.[12,15] The surface concentrations of DAPV, DADD, and $RuL_2(NCS)_2$ were in the same order of magnitude of 4.0×10^{-10}–9.0×10^{-10} mol cm^{-2} on ITO. The SAMs and Ru complex formed quite dense molecular layers in the range of 3–5 molecules per nm^2. The dyad was stable enough to be fabricated in air or aqueous media. The self-assembly technique proved an efficient method to construct the molecular architecture on the ITO surface.

(2) Photoinduced electron transfer and ITO conductivity change

For efficient photoinduced electron transfer, the proper arrangement of energy levels in the dyad is very important. Scheme 2 shows an idealized arrangement of dyad on the ITO surface and the energy level alignment of di-(3-diaminopropyl)-viologen (DAPV), $RuL_2(NCS)_2$, and ITO. The LUMO of $RuL_2(NCS)_2$ is at −3.8 eV, and ITO at −4.7 eV. The reduction potential of DAPV is −4.0 eV, which bridges the energy gap between $RuL_2(NCS)_2$ and ITO. The energy level alignment with an appropriate bridging unit facilitates electron transfer from the LUMO of the Ru complex into ITO. Facile electron transfer will change the electron density in ITO, which induces a change in the ITO conductivity. Therefore, the photoconductivity changes in ITO are directly related to the bridging capability of the electron acceptors between the Ru complex and ITO.

To examine the capability of SAMs bridging the photoinduced electron transfer, ITO conductivity was measured with and without the viologen moiety (Scheme 2a). In order to monitor the maximum conductivity change upon illumination, low conductivity ITO (1 kΩ cm) was used as a base material. As shown in Fig. 4, the $RuL_2(NCS)_2$–DAPV–ITO system exhibits drastic changes in conductivity. The currents through the ITO surface increased by 8 nA under illumination (89 mW cm^{-2}), and returned back to its original position when the light is off. The photoresponse phenomenon was repeated regularly. The mechanism for the observed conductivity change is suggested in Scheme 2b. The irradiated photon excites the Ru complex, and thee photo-excited electrons of $RuL_2(NCS)_2$ are transferred to low-lying energy state of DAPV (−4.0 eV). The energy level of ITO is –4.7 eV, and electrons in DAPV will spontaneously move to ITO. As a result, the electron density of

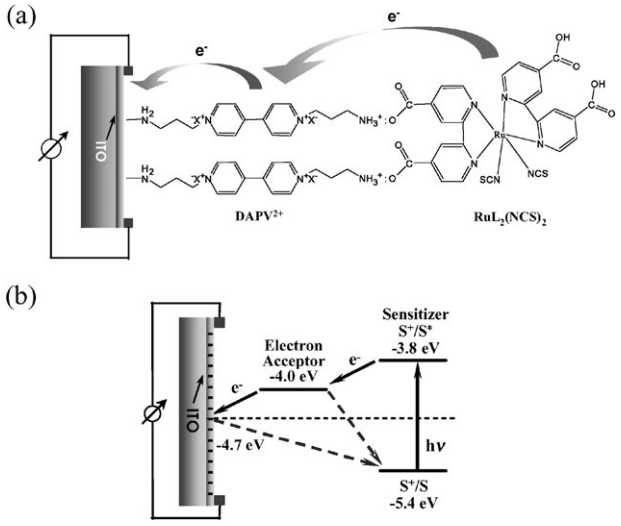

Scheme 2 Idealized photoinduced electron transfer and conductivity measurement; (a) schematic diagram of the electron acceptor–sensitizer dyad on ITO, (b) energy level diagram and electron transfer through the dyad.

ITO increases and its conductivity increases. Under dark conditions, the whole system returns to the initial state decreasing the conductivity. The oxidized $RuL_2(NCS)_2$ can be reduced by recombination or by air environment. The conductivity change is more significant in air than in a vacuum, because air partly supplies electrons to the photo-oxidized Ru complexes, providing more electrons to the ITO than a vacuum. In a vacuum environment, the recombination step is the main route to reduce the oxidized $RuL_2(NCS)_2$. The drift in over the course of time is attributed to the temperature change of the ITO surface due to the irradiation. Meanwhile, the photosensing effects were not observed without the viologen moiety in SAMs–ITO ($RuL_2(NCS)_2$–DADD–ITO, $RuL_2(NCS)_2$–ITO, and bare ITO). For that reason, the presence of a viologen unit as an electron acceptor is essential for the photosensing effects. Similar to what occurs in the photosynthetic system in nature, the energy level alignment of the electron acceptors and sensitizer is essential for the high photon-energy conversion. The SAMs of $RuL_2(NCS)_2$–DAPV on ITO are a prototype mimicking the photosynthetic system in nature.

Cyclic voltammetry was performed to examine the electronic states of the Ru complexes in the presence of the viologen moiety. The $RuL_2(NCS)_2$ complex shows a characteristic Ru(II)/Ru(III) oxidation peak at 850 mV (*vs.* SCE) in acetonitrile. The $RuL_2(NCS)_2$ on SAMs–ITO or ITO has two oxidation

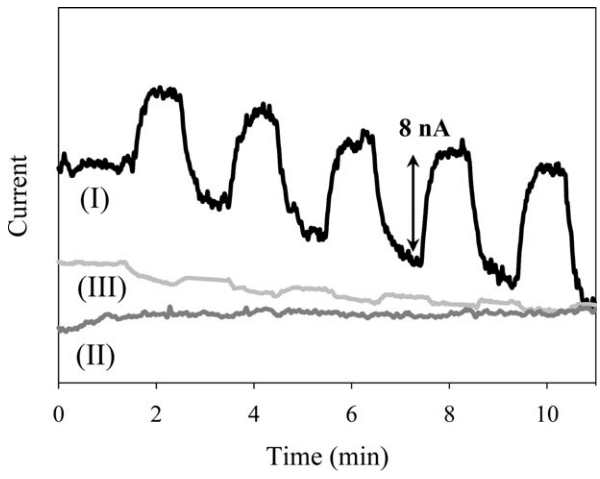

Fig. 4 Photoinduced current change of (I) $RuL_2(NCS)_2$–DAPV dyad on ITO, (II) $RuL_2(NCS)_2$ on ITO, and (III) Bare ITO.

reactions: Ru(II)/Ru(III) at 800 mV and Ru(III)/Ru(IV) at 1235 mV (Fig. 5a, (II)). However, the $RuL_2(NCS)_2$ with DAPV on ITO shows a new oxidation peak at 1110 mV under illumination (Fig. 5a, (I)). This indicates a change in the Ru oxidation state upon illumination. Upon irradiation, metal to ligand electron transfer will take place followed by transfer to the electron acceptor. The peak change indicates electron transfer from the metal to the acceptor system. The Ru oxidation state was independently monitored by a chemical oxidation with Ce(IV) sulfate, which is an oxidizing agent (eqn. (1)). Rhee *et al.* reported that Ce(IV) can oxidize Ru(II) to Ru(III).[10]

$$Ru(II)L_2(NCS)_2 + Ce(IV) \rightarrow Ru(III)L_2(NCS)_2 + Ce(III) \quad (1)$$

$$2Ru(III)L_2(NCS)_2 + 3I^- \rightarrow 2Ru(II)L_2(NCS)_2 + I_3^- \quad (2)$$

Interestingly, the oxidation peak of the chemically oxidized Ru(III) complex is exactly the same as the one of $RuL_2(NCS)_2$–DAPV–ITO under irradiation. This indicates that photoxidation took place from Ru(II) to Ru(III) upon irradiation, and the oxidation peak at 1110 mV represents the oxidation process of Ru(III)/Ru(IV). The photo illumination oxidizes Ru(II) $L_2(NCS)_2$ to Ru(III)$L_2(NCS)_2$ in the presence of a viologen unit. The electrons in the HOMO of $RuL_2(NCS)_2$ are photo-excited to the LUMO and transferred to the viologen, and then to ITO. However, the cyclic voltammogram of $RuL_2(NCS)_2$–DADD–ITO was not changed and remained in the Ru(II) state even upon illumination (Fig. 5b). The chemical oxidation of $RuL_2(NCS)_2$–DADD–ITO by Ce(IV) produces a Ru(III) complex and showed the same cyclic voltammogram as the Ru(III) complex with DAPV under illumination. The photo-oxidation of the $RuL_2(NCS)_2$ complex was not observed without the viologen bridging group. The DADD consists of covalent bonds and acts as an insulator. Therefore, it is difficult for the photo-excited electrons in $RuL_2(NCS)_2$ to cross covalent bonds, and they return to the ground state, Ru(II). The presence of a bridging component between the sensitizer and ITO facilitates electron transfer, and is an essential part for the electron flow. The reduction peak of the viologen at −600 mV decreases when irradiated. The viologen is partially reduced as a result of electron transfer from the ruthenium sensitizer. The addition of I^-, an electron injector (−4.8 eV), provides electrons to the photo-oxidized Ru(III) complex to form a Ru(II) complex (Fig. 5c, eqn. (2)). The cyclic voltammogram of $RuL_2(NCS)_2$–DAPV–ITO shows the recovery of the Ru(II) state in the presence of I^- even under irradiation conditions. The oxidation state changes in the Ru(II)$L_2(NCS)_2$ complexes upon illumination suggest that the viologen moiety plays a crucial role in bridging the LUMO of $RuL_2(NCS)_2$ and ITO energetically.

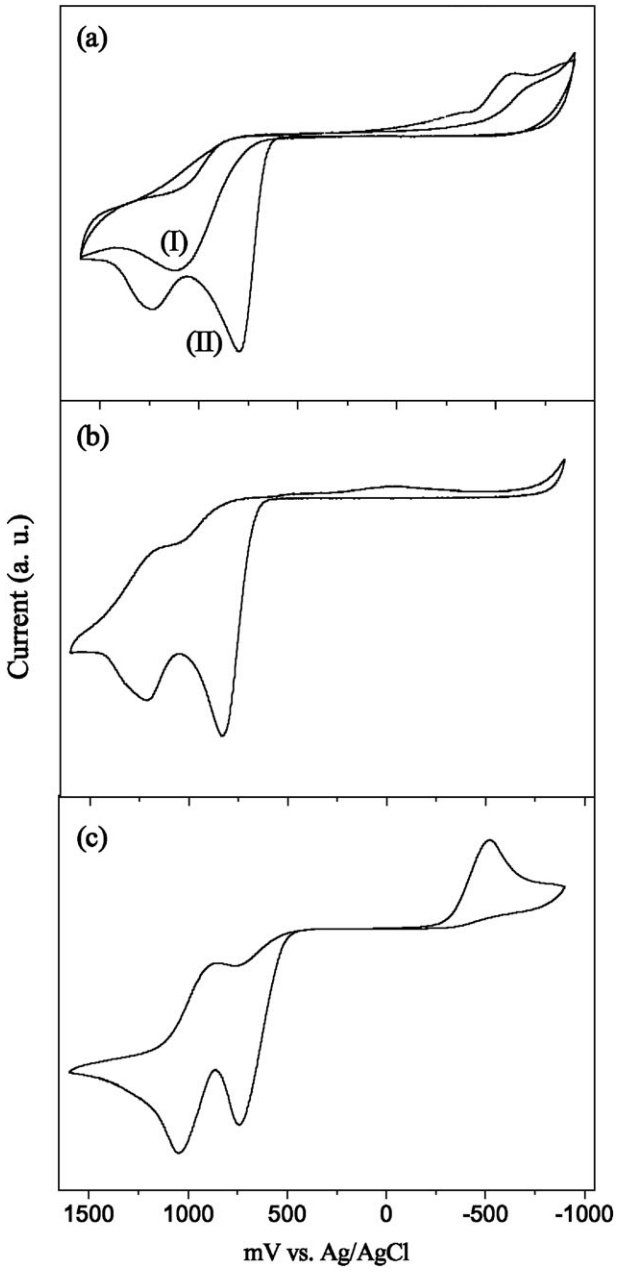

Fig. 5 Cyclic voltammogram of $RuL_2(NCS)_2$–SAMs–ITO in 0.1 M $(Bu)_4NBF_4$–CH_3CN as electrolyte at a scan rate of 550 mV s^{-1}; (a) in the case of DAPV SAMs in the dark (I) and under illumination (II); (b) in the case of DADD SAMs in the dark or under illumination; (c) in the case of DAPV SAMs with I^- in 0.1 M $(Bu)_4NBF_4$–CH_3CN in the dark or under illumination.

(3) Molecular photovoltaic system with SAMs of acceptor and sensitizer on ITO

The molecular photovoltaic system is an idealized model for unidirectional electron transfer upon irradiation. By the proper arrangement of acceptor–sensitizer–donor molecules on ITO, photoinduced electron flow can be obtained and optimized. The formation of the SAMs with the alignment of the acceptor–sensitizer energy level on the ITO was further used to construct the molecular photovoltaic devices. A sandwich-type photovoltaic device was prepared with the $RuL_2(NCS)_2$–DAPV–ITO and a platinum counter electrode with an electrolyte of 0.3 M LiI and 0.03 M I_2 in acetonitrile. The photoactive spectrum of the ITO–DAPV–$RuL_2(NCS)_2$/(I^-/I_3^-)/Pt cell accords with the corresponding UV-Vis absorption spectrum in $RuL_2(NCS)_2$ solution. It shows a maximum absorbance at 530 nm. In the presence of an electron mediator, viologen in SAMs, the incident photon to electron current quantum efficiency (IPCE) of $RuL_2(NCS)_2$ is higher than that without a viologen unit (Fig. 6).[19] DADD and DAPV are similar in their length. However, the IPCE increases by almost three times with an energetically bridging unit. This striking improvement is due largely to the promotion of electron transfer by the bridging viologen moiety between $RuL_2(NCS)_2$ and ITO.

Based on the IPCE experiments, the photocurrents were measured under monochromatic irradiation ($\lambda = 530$ nm; light intensity, 3.3 mW cm^{-2}; area, 0.34 cm^2). Two systems were compared to each other: ITO–DAPV–$RuL_2(NCS)_2$, and ITO–DADD–$RuL_2(NCS)_2$. In both cases, there was a photocurrent upon irradiation. However, the system performance in the presence of the viologen moiety shows an excellent performance (Fig. 7). The open-circuit voltage (V_{oc}) of the $RuL_2(NCS)_2$ with a viologen acceptor reaches 0.17 V with a short-circuit current (J_{sc}) of 1.7 μA cm^{-2}, whereas the $RuL_2(NCS)_2$–DADD–ITO system shows a poor V_{oc} of 0.015 V, and especially its J_{sc} is 15 times smaller than that of $RuL_2(NCS)_2$–DAPV–ITO. The photo-excited electrons in

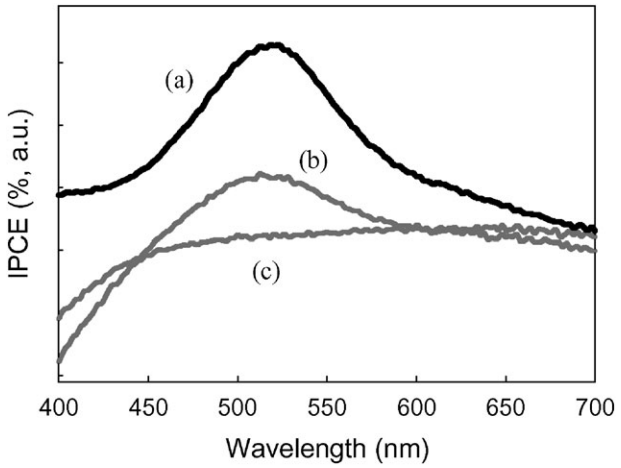

Fig. 6 Incident photon-to-current conversion efficiency (IPCE). (a) $RuL_2(NCS)_2$–DAPV–ITO; (b) $RuL_2(NCS)_2$–DADD–ITO; (c) bare ITO.

$RuL_2(NCS)_2$ are transferred to the viologen in SAMs on ITO. Then, electrons will travel to the ITO side, the same as in the previous photosensor experiments. On the other hand, the $RuL_2(NCS)_2$ complex oxidized Ru to the Ru(III) state. The electrolyte with I^-/I_3^-, a redox mediator, provides electrons to the Ru(III) and I_3^-, and the system returns to its original Ru(II) state. At the counter electrode, I^- is regenerated from I_3^- by accepting electrons from the electrode. The electron transfer from reduced-viologen to ITO is sufficiently fast due to the short distance of 3 methylene groups between viologen and ITO. However, there are 12 methylene groups in the DADD molecule, and it acts as a barrier to electron transfer.

The quantum yield, which is the ratio of generated electrons to absorbed photons, was 18.4% for $RuL_2(NCS)_2$–DAPV–ITO. Ikeda, *et al.* prepared multilayers of fullerene-cationic homooxacalix[3]arene inclusion complex with an anionic porphyrin polymer.[22a] They reported a good quantum yield of 21% under 1.53 mW cm^{-2} irradiation. Imahori, *et al.* also reported the formation of ferrocene-porphyrin-fullerene triad on gold surface. They prepared the triad by the multi-step organic synthesis and put it on the gold surface. They claimed the highest quantum yield of 25% under the irradiation power of 0.06 mW cm^{-2}.[20b,c] The quantum yield is directly dependent on the irradiation power. The quantum yield of 18.4% and photocurrent of 1.7 μA cm^{2-} under 3.3 mW cm^{-2} illumination conditions is a relatively good value among the recently reported systems.[3,21,22] The DADD SAMs without an electron acceptor behave as insulators between the $RuL_2(NCS)_2$ and ITO, and its quantum yield is almost negligible. The quantum efficiency was also calculated to be 0.1% with 1.7 μA cm^{-2} under 3.3 mW cm^{-2} ($\lambda_{ex} = 530$ nm).[19] The values provide good potential for a practical system of a molecular photovoltaic system.

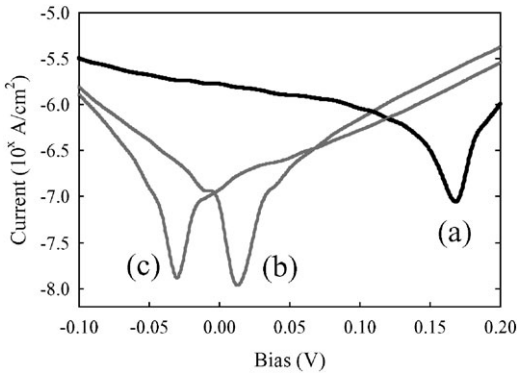

Fig. 7 *I–V* characteristics of the photovoltaic cells. (a), (c) $RuL_2(NCS)_2$–DAPV–ITO under irradiation and in the dark, respectively; (b) $RuL_2(NCS)_2$–DADD–ITO under irradiation.

The concept of molecular photovoltaic systems with SAMs of di-(3-diaminopropyl)-viologen shows good cell performance with an improved quantum yield. The system reported in this work provides a typical model for the molecular optoelectronic system. First, it is easily prepared on the ITO surface with excellent stability. Also, the architecture can be constructed by the layer-by-layer method in liquid phase. The formation of an acceptor–sensitizer dyad with di-(3-diaminopropyl)-viologen and $RuL_2(NCS)_2$ clearly shows its advantages with good cell performance. The elaborated fine-tuning of the energy level of acceptors and sensitizers, and their multilayers will provide us an outstanding methodology for designing optoelectronics on ITO.

Sumamry

In summary, a molecular photosensor based on self-assembled monolayers of an electron acceptor–photosensitizer dyad on an ITO surface was fabricated. The energy level alignment through the SAMs of di-(3-diaminopropyl)-viologen successfully facilitates electron transfer and alters the ITO conductivity. The concept of a molecular photosensor was applied to a molecular photovoltaic system with a good quantum yield of 18.4%. The formation of self-assembled layers of an acceptor–sensitizer dyad on ITO is an attractive model for molecular optoelectronics mimicking photosynthesis.

References

1 N. Liu, Z. Chen, D. R. Dunphy, Y. B. Jiang, R. A. Assink and C. J. Brinker, *Angew. Chem., Int. Ed.*, 2003, **42**, 1731–1734.
2 M. Grätzel, *Nature*, 2001, **414**, 338–344.
3 H. Yamada, H. Imahori, Y. Nichimura, I. Yamazaki, T. K. Ahn, S. K. Kim, D. H. Kim and S. Fukuzumi, *J. Am. Chem. Soc.*, 2003, **125**, 9129–9139.
4 I. A. Banerjee, L. Yu and H. Matsui, *J. Am. Chem. Soc.*, 2003, **125**, 9542–9543.
5 S. Sortino, S. Petralia, S. Conoci and S. D. Bella, *J. Am. Chem. Soc.*, 2003, **125**, 1122–1123.
6 M. Hervás, J. A. Navarro and M. A. De La Rosa, *Acc. Chem. Res.*, 2003, **36**, 798–805.
7 A. Ben-Shem, F. Frolow and N. Nelson, *Nature*, 2003, **426**, 630–635.
8 P. Jordan, P. Fromme, H. T. Witt, O. Klukas, W. Saenger and N. Krauß, *Nature*, 2001, **411**, 909–917.
9 A. Zouni, H. T. Witt, J. Kern, P. Fromme, N. Krauß, W. Saenger and P. Orth, *Nature*, 2001, **409**, 739–743.
10 K. H. Rhee, E. P. Morris, J. Barber and W. Kühlbrandt, *Nature*, 1998, **396**, 283–286.
11 S. Y. Oh, Y. J. Yun, D. Y. Kim and S. H. Han, *Langmuir*, 1999, **15**, 4690–4692.
12 S. Y. Oh, Y. J. Yun, D. Y. Kim, K. H. Hyung and S. H. Han, *New J. Chem.*, 2004, **28**, 495–501.
13 S. Y. Oh and S. H. Han, *Langmuir*, 2000, **16**, 6777–6779.
14 S. Y. Oh and S. H. Han, *Synth. Met.*, 2001, **121**, 1369–1370.
15 K. H. Hyung and S. H. Han, *Synth. Met.*, 2003, **137**, 1441–1142.
16 X. Y. Tang, T. W. Schneider, J. W. Walker and D. A. Buttry, *Langmuir*, 1996, **12**, 5921–5933.
17 P. M. S. Monk, *Dyes Pigm.*, 1998, **39**, 125–128.
18 T. Sagara, H. Maeda, Y. Yuan and N. Nakashima, *Langmuir*, 1999, **15**, 3823–3830.
19 In *Physics of Semiconductor Devices*, ed. S. M. Sze, Wiley-Interscience, New York, 1981, ch. 12, pp. 640–683.
20 (*a*) D. M. Guldi, F. Pellarini, M. Prato, C. Granito and L. Troisi, *Nano Lett.*, 2002, **2**, 965–968; (*b*) H. Imahori, H. Yamada, Y. Nishimura, I. Yamazaki and Y. Sakata, *J. Phys. Chem. B*, 2000, **104**, 2099–2108; (*c*) H. Imahori, H. Yamada, S. Ozawa, K. Ushida and Y. Sakata, *Chem. Commun.*, 1999, 1165–1166.
21 (*a*) C. Luo, D. M. Guldi, M. Maggini, E. Menna, S. Mondini, N. A. Kotov and M. Prato, *Angew. Chem., Int. Ed.*, 2000, **39**, 3905–3909; (*b*) K. Uosaki, T. Kondo, X. Q. Zhang and M. Yanagida, *J. Am. Chem. Soc.*, 1997, **119**, 8367–8368.
22 (*a*) A. Ikeda, T. Hatano, S. Shinkai, T. Akiyama and S. Yamada, *J. Am. Chem. Soc.*, 2001, **123**, 4855–4856; (*b*) A. Terasaki, T. Akiyama and S. Yamada, *Langmuir*, 2002, **18**, 8666–8671; (*c*) T. Akiyama, S. Nitahara, S. Inoue and S. Yamada, *Photochem. Photobiol. Sci.*, 2004, **3**, 26–28.